

Mechanical Characterizations of Boron Oxide Doped Ytria-stabilized Tetragonal Zirconia Electrolyte for High-temperature Solid Oxide Fuel Cell Operated

Abeer Farouk Al-Attar¹, Mohamed J. Eshraghi², Saad B. H. Farid¹ and Fadel A. Hashim¹

¹Department of Materials Engineering, University of Technology, Baghdad-Iraq

²Materials and Energy Research Center (MERC), Karaj, Iran

Abstract–The aim of this work is to estimate the effect of doping boron oxide to yttria-stabilized tetragonal zirconia (B₂O₃-Y-TZP) as electrolyte for solid oxide fuel cell operated at high temperature. Nanoindentation has been performed to investigate mechanical properties of doping and pure electrolyte, whereas scanning electron microscopy has been used for morphology studies of the sintered specimens, and X-ray diffraction used for identifying phase and microstructure of electrolyte. The crystallite size of B₂O₃ doped Y-TZP and Y-TZP estimated to be 137 nm and 895 nm, respectively. The grain size of B₂O₃ doped Y-TZP and Y-TZP was estimated to be 426 nm and 1225 nm, respectively. B₂O₃ doped Y-TZP specimens exhibited elastic modulus (E) 115E+15 Pa with yield stress t (N/m²) as much as 327.198 MPa, hardness as much as 948.623 kg/mm², and fracture strength as much as 3.421 MPa.M^{1/2}.

Index Terms–Boron oxide, High-temperature Solid oxide fuel cell operated, Mechanical properties, Nanoindentation, Ytria-stabilized tetragonal zirconia.

I. INTRODUCTION

Nanoindentation is recognized as a technique to characterize the mechanical properties of materials at very small scales or ultralow applied load indentation [1]. Y₂O₃-stabilized zirconia is well known for its high hardness, toughness, and strength [2]. Previous experimental results show that boron oxide (B₂O₃) facilitated phase transformation from cubic to monoclinic phase [3]. In addition, B₂O₃ is known as a glass former [4]. To the author knowledge, there is no report on the mechanical properties of B₂O₃ doped Y-TZP. Therefore, in the current work, sintered 2 mol% B₂O₃ doped Y-TZP pellets have been manufactured and its mechanical properties

have been estimated by nanoindentation examination with a diamond cube-corner indenter.

II. EXPERIMENTAL PART

About 3 mol% TZP nanopowder supplied by Hongwu International Group Ltd., China, B₂O₃ and stearic acid supplied by Merck used as raw materials. The X-ray diffraction (XRD) and scanning electron microscopy (SEM) of raw materials analyzed to determine their phases and particle size.

The XRD pattern of raw materials and sintered specimens was taken using Philips analytical XRD type PW1930 with cobalt $\lambda_{\text{Co}} = 1.78901 \text{ \AA}$ radiation tube operating at 40 kV and 30 mA. The particle size determined by SEM TESCAN Vega III Czech Republic used 5 KV to get the image in Fig. 1. Doped specimens prepared by mixing 2 mol% B₂O₃ in 99.987 purity with Y-TZP in Spex 6000 Mixer/Miller with zirconia jars and zirconia balls with different sizes in diameter range from 10 to 18 mm for 60 min. The mixtures were compacted by cold pressing at 27.50 MPa in stainless steel die 20 mm in diameter and 0.6 mm thick. Green specimens sintered in air using a Retsch box furnace at 1923°K. To make sure that specimens undergo slow heating and to avoid thermal stress during sintering the heating rate kept at 2°K/min. The heating profile depicted in Fig. 2.

The specimens kept for 1 h at 673°K to make sure of removed binder and kept for 1 h at 1100°K and finally sintered at 1923°K for 180 min as shown in Fig. 2. The morphology of specimens examined by SEM Cambridge with 10.0X resolution after polishing and 15 min thermal etching at 1673°K and sputter coating with Au. XRD used to identify the phase, crystal structure, and crystallite size of sintered specimen. The mechanical properties of sintered specimens estimated by nanoindentation tester type Triboscope system; model Hysitron at room temperature carried out with International Standards Organization (ISO) 14577 with a cube-corner indenter with average radius of curvature <50 nm. The tip of the testing instrument was calibrated by Oliver-Pharr method (ISO 14577) [5,6]. The procedure performed done with applied indenter tip with increasing normal load

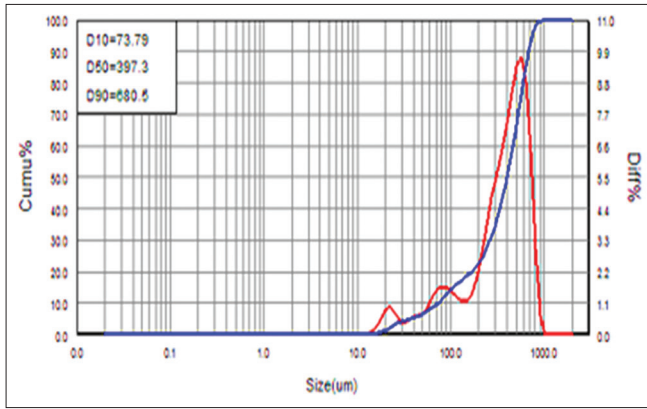


Fig. 1. Scanning electron microscopy of yttria-stabilized tetragonal zirconia powder.

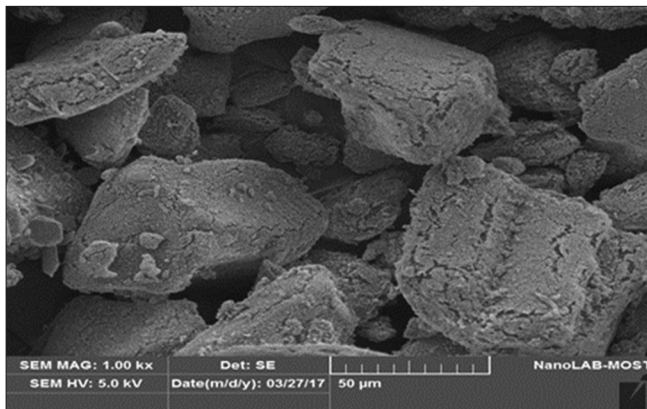


Fig. 2. Heating profile for sintering pellets

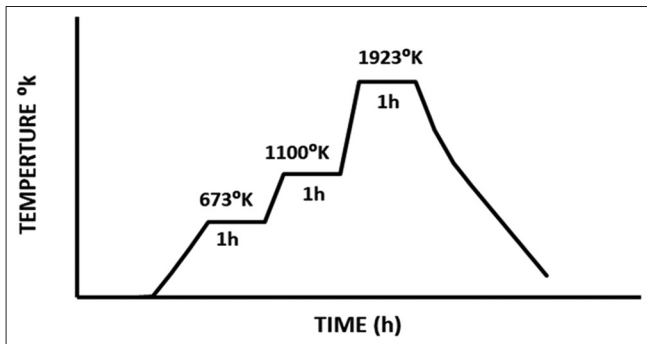


Fig. 3. Particle size analysis of boron oxide.

on the surface of the tester specimen. When the penetration depth of tip indenter reached a preset maximum value, the normal load will be gradually reduce until partial or complete relaxation occurs [7]. In the current work, the P_{max} load ranges from 908.8 to 984.5 μN , which applied at fixed rate of about 196.9 $\mu\text{N/S}$. The nanomechanical properties of the B_2O_3 doped Y-TPZ such as reduced elastic modulus and hardness, evaluated from the load-displacement nanoindentation data using the widely accepted Oliver and Pharr method [8,9]. The young modulus calculated using eq. (1):

$$\frac{1}{E_r} = \frac{1-\nu^2}{E} + \frac{1-\nu_i^2}{E_i} \quad (1)$$

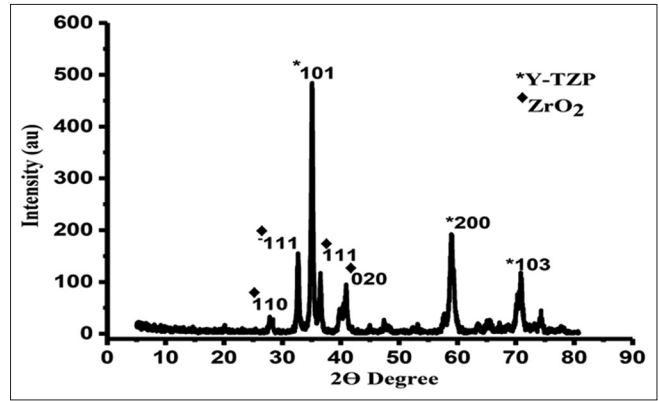


Fig. 4. X-ray diffraction pattern of yttria-stabilized tetragonal zirconia powders.

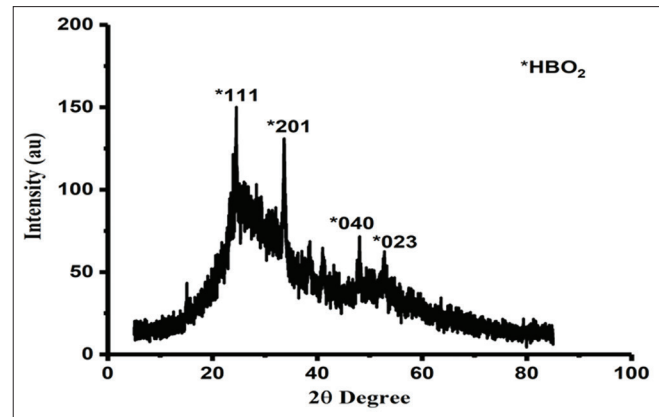


Fig. 5. X-ray diffraction pattern of HBO2 powders.

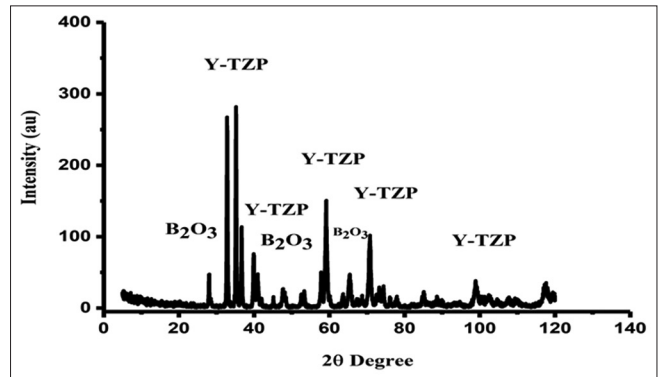


Fig. 6. X-ray diffraction data for sintered yttria-stabilized tetragonal zirconia.

Where, E_r is reduced elastic modulus, ν is Poisson ratio for the endurance material, and E_i and ν_i are the elastic modulus and Poisson ratio of the indenter, respectively. The hardness was evaluated from eq. (2):

$$H = \frac{P_{max}}{A} \quad (2)$$

Where, A : Contact area at that load, P_{max} : Maximum load, and the stiffness (S) was estimated from eq. (3) [10]:

$$E_r = \frac{\sqrt{\pi} S}{2 \sqrt{A}} \quad (3)$$

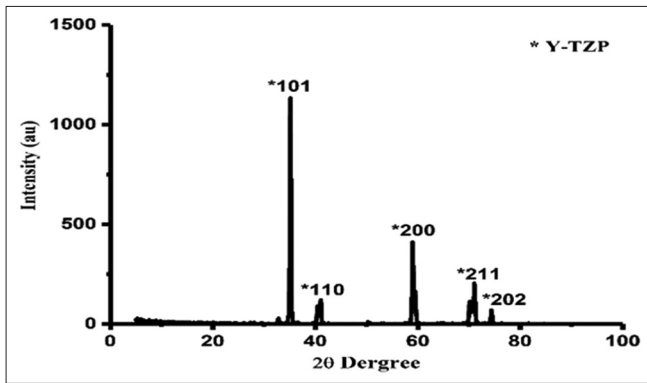


Fig. 7. X-ray diffraction date for sintered boron oxide doped yttria-stabilized tetragonal zirconia.

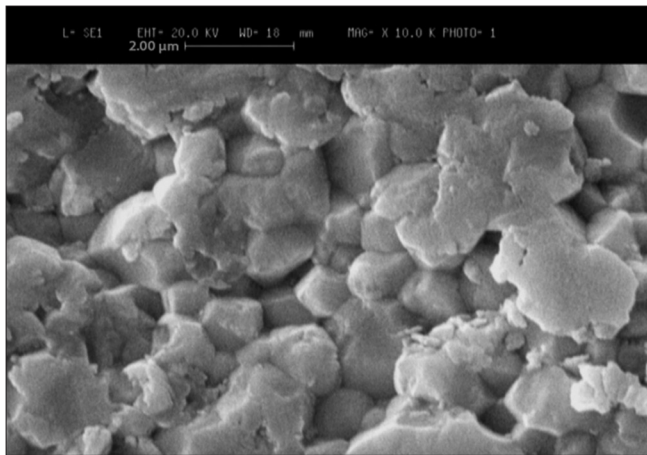


Fig. 8. Sintered yttria-stabilized tetragonal zirconia at 1893°K.

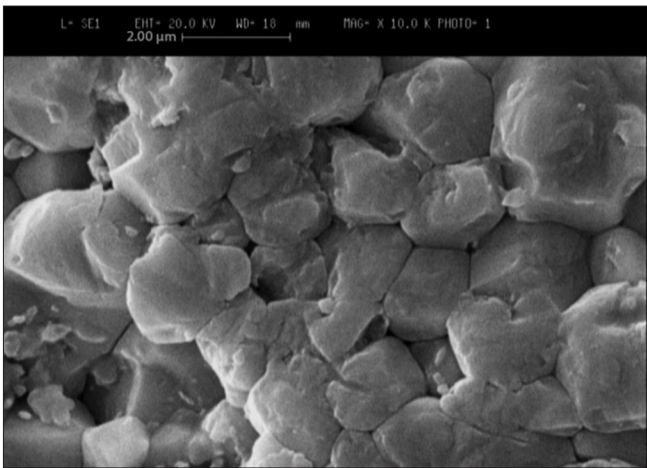


Fig. 9. Sintered boron oxide doped yttria-stabilized tetragonal zirconia at 1893°K.

III. RESULTS AND DISCUSSION

Fig. 3 shows the particle size of B_2O_3 , while in Fig. 1, the particle size of Y-TZP can be seen. In Fig. 4, XRD pattern of Y-TZP powders is shown. In addition to Y-TZP phase, a small amount of ZrO_2 impurity phases is also present. Fig. 5 shows the XRD pattern of as received B_2O_3 powders which exhibit HBO_3 phase. This could be as a result of humidity of the powder during delivery for the XRD analysis.

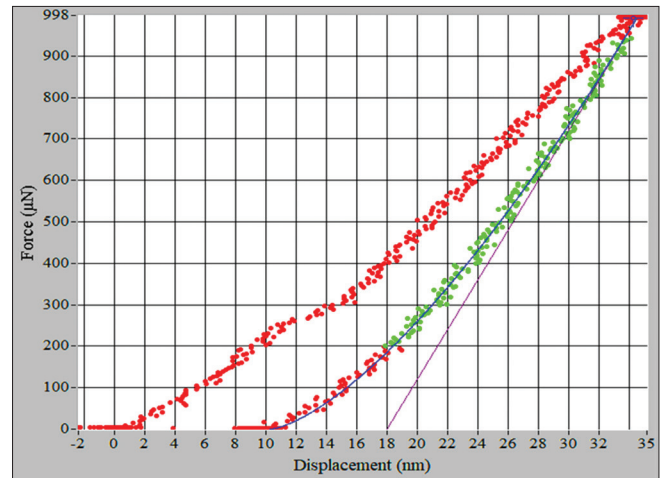


Fig. 10. Load-displacement curve (P-h) of yttria-stabilized tetragonal zirconia.

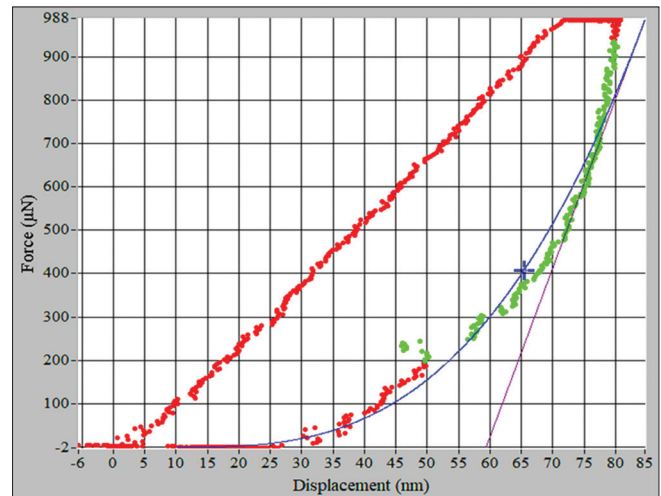


Fig. 11. Load-displacement curve (P-h) of boron oxide-yttria-stabilized tetragonal zirconia

Fig. 6 shows XRD date of the sintered powder of Y-TZP. On the other hand, Fig. 7 shows small peaks of B_2O_3 and substantial peaks of Y-TZP doped B_2O_3 in the same sintered specimen.

Williamson-Hall analysis showed that the peak broadening is mostly due to the crystallite size [11]. Based on this analysis, the crystallite size of Y-TZP was estimated to be around 137 nm.

$$B \times \cos(\theta) = \frac{K \times \lambda}{\text{Size}} + 4 \times \text{Strain} \times \sin(\theta) \quad (4)$$

In Figs. 8 and 9, SEM micrographs of sintered Y-TPZ and B_2O_3 to yttria-stabilized tetragonal zirconia (B_2O_3 -Y-TZP) were shown. It can be noticed that the doped Y-TZP shows grain growth in comparison to pure Y-TPZ due to the effect of 2%mol B_2O_3 . The average grain size of sintered Y-TPZ is about 426 nm, while the B_2O_3 doped Y-TZP is about 1225 nm.

The elasticity modulus of Y-TPZ and B_2O_3 -Y-TPZ can be calculated using eq. (1) in load-displacement curve for both Figs. 10 and 11 as listed in Table I.

TABLE I ESTIMATED MECHANICAL PROPERTIES THROUGH NANOINDENTATION TECHNIQUE FOR SINTERED PELLETS

Specimen code	Elastic modulus (E) (Pa)	Hardness (H) (kg/mm ²)	Yield stress σ (N/m ²)	Fracture strength (MPa.M ^{1/2})	Crystal size (nm)
Y-TZP	759E+15	8188.603	2823.656	3.085	137
B ₂ O ₃ -Y-TZP	115E+15	948.623	327.198	3.421	895

B₂O₃-Y-TZP: Boron oxide to yttria-stabilized tetragonal zirconia

From Table I, it can be observed that B₂O₃ caused reduction in elastic modulus, hardness, and yield stress, while resulted in improvement in stiffness fracture strength.

IV. CONCLUSION

The influence of B₂O₃ content on the densification, tetragonal phase stability, young modulus, hardness, and fracture toughness was investigated using nanoindentation technique. Morphology of the sintered specimens was obtained through SEM, whereas the phases of both mixtures and sintered doping Y-TZP specimens were characterized by XRD.

V. ACKNOWLEDGMENTS

The authors thank Materials and Energy Research Center in Iran for the completion of the practical part of this paper.

REFERENCES

- [1] D. W. Stollberg, J. M. Hampikian, L. Riester and W. B. Carter, "Nanoindentation measurements of combustion CVD Al₂O₃ and YSZ films," *Materials and Engineering*, vol. A359, pp. 112-118, 2003.
- [2] A. Paul, B. Vaidhyanathan and J. G. P. Binner, "Hydrothermal aging behavior of nanocrystalline Y-TZP ceramics," *Journal of the American Ceramic Society*, vol. 94, pp. 2146-2152, 2011.
- [3] J. Clerk Maxwell, *A Treatise on Electricity and Magnetism*, 3rd ed., vol. 2. Oxford: Clarendon, 1892, pp. 68-73.
- [4] D. Z. de Florio and R. Muccillo, "Effect of boron oxide on the cubic-to-monoclinic phase transition in yttria-stabilized zirconia," *Materials Research Bulletin*, vol. 39, pp. 1539-1548, 2004.
- [5] S. Ghosh, A. D. Sharma, P. Kundu and R. N. Basu, "Glass-ceramic sealants for planar IT-SOFC: A bilayered approach for joining electrolyte and metallic interconnect," *Journal of The Electrochemical Society*, vol. 155, pp. B473-B478, 2008.
- [6] Metallic Materials-Instrumented Indentation Test for Hardness and Materials Parameters. "Verification and Calibration of Testing Machines". Part 2. Geneva, Switzerland: International Organization for Standards, 2002.
- [7] W. C. Oliver and G. M. Pharr, "Measurement of hardness and elastic modulus by instrumented indentation: Advances in understanding and refinements to methodology," *Journal of Materials Research*, vol. 19, pp. 3-20, Jan, 2004.
- [8] A. Karimzadeh, M. R. Ayatollahi and H. A. Shirazi, "Mechanical properties of a dental nano-composite in moist media determined by nano-scale measurement," *International Journal of Materials, Mechanics and Manufacturing*, vol. 2, no. 1, Feb, pp. 67-72, 2014.
- [9] M. Fujikane, D. Setoyama, S. Nagaob, R. Nowak and S. Yamanaka, "Nanoindentation examination of yttria-stabilized zirconia (YSZ) crystal," *Journal of Alloys and Compounds*, vol. 431, pp. 250-255, 2007.
- [10] M. Keshavarz, M. H. Idris, N. Ahmad, "Mechanical properties of stabilized zirconia nanocrystalline EB-PVD coating evaluated by micro and nano indentation," *Journal of Advanced Ceramics*, vol. 2, pp. 333-340, 2013.
- [11] V.D. Mote, Y. Purushotham and B.N. Dole, "Williamson-Hall analysis in estimation of lattice strain in nanometer-sized ZnO particles," *Journal of Theoretical and Applied Physics*, vol. 6, pp. 1-8, 2012.